JOURNAL OF VIROLOGY, Feb. 1997, p. 1341–1352 Vol. 71, No. 2
0022-538X/97/$04.00+0

Subcellular Compartmentalization of Adeno-Associated Virus Type 2 Assembly

ANDREAS WISTUBA, ANDREA KERN, STEFAN WEGER, DIRK GRIMM, AND JÜRGEN A. KLEINSCHMIDT*

Deutsches Krebsforschungszentrum, Forschungsschwerpunkt Angewandte Tumorvirologie, D-69120 Heidelberg, Germany

Received 12 July 1996/Accepted 28 October 1996

Using immunofluorescence and in situ hybridization techniques, we studied the intracellular localization of adeno-associated virus type 2 (AAV-2) Rep proteins, VP proteins, and DNA during the course of an AAV-2/adenovirus type 2 coinfection. In an early stage, the Rep proteins showed a punctate distribution pattern over the nuclei of infected cells, reminiscent of replication foci. At this stage, no capsid proteins were detectable. At later stages, the Rep proteins were distributed more homogeneously over the nuclear interior and finally became redistributed into clusters slightly enriched at the nuclear periphery. During an intermediate stage, they also appeared at an interior part of the nucleolus for a short period, whereas most of the time the nucleoli were Rep negative. AAV-2 DNA colocalized with the Rep proteins. All three capsid proteins were strongly enriched in the nucleolus in a transient stage of infection, when the Rep proteins homogeneously filled the nucleoplasm. Thereafter, they became distributed over the whole nucleus and colocalized in nucleoplasmic clusters with the Rep proteins and AAV-2 DNA. While VP1 and VP2 strongly accumulated in the nucleus, VP3 was almost equally distributed between the nucleus and cytoplasm. Capsids, visualized by a conformation-specific antibody, were first detectable in the nucleoli and then spread over the whole nucleoplasm. This suggests that nucleolar components are involved in initiation of capsid assembly whereas DNA packaging occurs in the nucleoplasm. Expression of a transfected full-length AAV-2 genome followed by adenovirus infection showed all stages of an AAV-2/adenovirus coinfection, whereas after expression of the cap gene alone, capsids were restricted to the nucleoli and did not follow the nuclear redistribution observed in the presence of the whole AAV-2 genome. Coexpression of Rep proteins released the restriction of capsids to the nucleolus, suggesting that the Rep proteins are involved in nuclear redistribution of AAV capsids during viral infection. Capsid formation was dependent on the concentration of expressed capsid protein.

The nucleus, commonly referred to as the control center of the eucaryotic cell, is highly organized into subcompartments to perform a number of essential functions such as DNA replication, RNA transcription, processing, and transport (6, 13, 58, 68). Development of protein and nucleic acid localization techniques allowed the visualization of many nuclear components and processes at discrete subnuclear sites, which suggests that they are part of an underlying structure involved in the functional organisation of the nucleus. These structures are highly dynamic and change in the cell cycle as a function of cellular activity (36, 39, 40, 43, 44, 54). Viral infections often are associated not only with a functional reprogramming of host cell gene expression but also with a reorganization of the cellular architecture, in particular of the nucleus (4, 9, 10, 14, 19, 20, 46, 56, 59, 64). Although several viral components possibly involved in formation and reorganization of this nuclear architecture are being investigated, they still are not well understood.

The life cycle of the adeno-associated virus (AAV) strongly depends on helper virus functions provided by either adenovirus or herpesvirus families (for reviews, see references 8 and 41). These helper viruses themselves show a profound influence on the host cells and a characteristic subcellular compartmentalization of viral products during infection (10, 46, 47, 49, 66). Coinfection of AAV-2 with adenovirus leads to induction of AAV-2 gene expression and to changes of the cellular milieu which are necessary for replication and production of infectious virus (3, 7, 11, 12, 15, 16, 31, 51). Accumulation of viral transcripts is controlled by a set of nonstructural AAV-2 proteins which are also required for DNA replication (5, 35, 38, 63). They are encoded by an overlapping reading frame located on the left half of the AAV-2 genome and are transcribed from either the p5 or the p19 promoter at map units 5 and 19, respectively. The transcripts from both promoters are translated from spliced and unspliced mRNAs, resulting in four proteins designated Rep78, Rep68, Rep52 and Rep40 according to their apparent molecular weight. Rep78 and Rep68 play key roles in AAV DNA replication (25, 62) by binding to the inverted terminal repeats and catalyzing the terminal resolution reaction (2, 29, 57). Several influences of these proteins on AAV gene expression have been documented, without delineating a comprehensive model for AAV gene regulation by these proteins (5, 27, 34, 35, 38, 63). Mutations that prevent the synthesis of the small Rep proteins Rep52 and Rep40 lead to a strongly reduced level of single-stranded DNA (ssDNA) accumulation, suggesting that they play a role in DNA packaging (17, 26). The AAV cap gene located in the right half of the AAV genome codes for three capsid proteins, VP1, VP2, and VP3, which are present in the virion in a 1:1:10 stoichiometry (32, 33, 52). Pulse-chase experiments support the view that the single-stranded AAV genomes are packaged into preformed capsids (42). In a time course of AAV-2/adenovirus type 2 coinfection, the synthesis of Rep and Cap proteins follows similar kinetics, reaching a maximum level around 20 h postin-

* Corresponding author. Mailing address: Deutsches Krebsforschungszentrum, Forschungsschwerpunkt Angewandte Tumorvirologie, Abteilung Tumorvirologie, Im Neuenheimer Feld 242, D-69120 Heidelberg, Germany. Phone: 49-6221-424978. Fax: 49-6221-424962. E-mail: j.kleinschmidt@dkfz-heidelberg.de.

fection together with bulk duplex DNA synthesis, whereas maximum ssDNA accumulation appears to occur about 4 h later (50). Immunoprecipitation experiments showed that Rep proteins were detected in complexes with capsid proteins possibly representing intermediates of the AAV-2 DNA packaging process (48, 67). The observation that the four Rep proteins colocalize in intranuclear centers together with the capsid proteins (28) was interpreted in terms of replication and packaging centers of AAV-2 DNA. Recently, it could be shown by in situ hybridization that AAV-2 DNA and Rep proteins colocalize with adenovirus DNA in common foci, which were interpreted as replication centers (65).

In this study, the dynamics of the subcellular distribution of AAV proteins, capsids, and DNA was monitored over the time course of an AAV-2/adenovirus type 2 coinfection to define the possible sites of AAV capsid assembly and DNA packaging. In early phases of infection, Rep proteins and AAV DNA are colocalized in typical replication centers, but at that time no capsid proteins were detectable, showing that these centers are not the sites of DNA packaging. By using a conformation-specific capsid antibody, it was possible to show that capsids accumulated first in the nucleoli and later also in intranuclear areas outside the nucleoli. Rep proteins and AAV DNA also colocalized in these extranucleolar zones, suggesting that DNA packaging could occur at these sites. DNA and Rep could hardly be detected in the nucleoli. Free capsid proteins, capsids, and Rep proteins underwent a number of redistributions during later stages of infection and showed mainly a separate nuclear localization. Expression of the *cap* and *rep* genes by transient transfection showed that capsid formation was strongly dependent on capsid protein concentration and that the Rep proteins have an influence on the subnuclear compartmentalization of AAV capsids.

MATERIALS AND METHODS

Cell culture and virus infections. HeLa cells were grown in Dulbecco's modified Eagle's medium (DMEM) supplemented with 10% fetal calf serum and penicillin-streptomycin at 37°C and 5% CO_2. For generation of AAV-2, cells were grown to 80% confluency, the medium was removed, and the cells were incubated with AAV-2 (multiplicity of infection [MOI] = 20) and adenovirus type 2 (MOI = 2) for 2 h in 2 to 3 ml of DMEM per 175-cm^2 flask. After the incubation period, DMEM was added and the cells were incubated at 37°C and 5% CO_2 for 3 days. Then the flasks containing cells and medium were frozen and thawed three times at −70 and 37°C, respectively. Debris was removed by centrifugation at 5,000 × g_{av}, and the clear supernatant was collected. Adenovirus was inactivated by heating to 56°C for 30 min. For generation of adenovirus stocks, HeLa cells were infected solely with adenovirus (MOI = 2) and supernatants were harvested as described above. AAV and adenovirus stocks were subjected to titer determination by immunofluorescence staining of cells which had been infected for 3 days either with serial dilutions of AAV to which adenovirus was added at an MOI of 2 or serial dilutions of adenovirus alone. Cells were grown to 70% confluency in 96-well plates prior to infection. AAV infections were monitored with monoclonal antibody 76/3 (67), which reacts with the nonspliced Rep proteins of AAV, and adenovirus infections were monitored with monoclonal antibody A30 (see below). Immunofluorescence staining was performed as described below, except that cells in 96-well plates were fixed with methanol alone before the staining procedure. The titers were calculated from the average numbers of fluorescence-positive cells infected with limiting dilutions of virus stocks.

For analysis of different stages of infection by immunofluorescence staining, cells were grown on coverslips and were infected in 10-cm petri dishes for 2 h in 1 ml of medium with the same MOIs as described for the preparation of virus stocks. After infection, 9 ml of medium was added and the dishes were incubated at 37°C and 5% CO_2 for the time intervals indicated at the respective experiments. Transfections of HeLa cells were performed in 10-cm petri dishes by following published protocols (18).

Plasmids. The plasmid containing the full-length AAV2 genome (pTAV-2) was derived from pAV-2 (37) as described previously (24). Plasmids designated pCMV-Rep78, pCMV-Rep68, pCMV-Rep52, and pCMV-Rep40 are identical to the respective plasmids pKEX-Rep78, pKEX-Rep68, pKEX-Rep52, and pKEX-Rep40 described elsewhere (27). The cap gene expression plasmid (pCMV-VP) was generated by insertion of a 650-bp *Bam*HI human cytomegalovirus (CMV) promoter fragment from pHCMV-Luci (kindly provided by K. Butz, German Cancer Research Center, Heidelberg, Germany) into the *Bam*HI site of BluescriptII SK+ (Stratagene) and ligation of the *Fsp*I-*Sna*BI cap gene fragment from pTAV-2 into the *Sma*I site of the same plasmid. pHCMV-Luci was constructed by cloning the *Hin*cII-*Ava*II fragment of the CMV promoter into the *Sma*I site of pUC19. An *Eco*RI-*Hin*dIII fragment containing the CMV promoter was subcloned into the *Eco*RI-*Hin*dIII site of plasmid pBL (21).

Gel electrophoresis, immunoblotting, and immunoprecipitation. Protein samples were analyzed on 15% polyacrylamide gels in the presence of sodium dodecyl sulfate (SDS-PAGE) (61). Total-cell lysates were prepared by sonification of cells in protein sample buffer followed by heating to 100°C for 5 min. For immunoblotting, proteins were electrophoretically transferred to nitrocellulose membranes by using a semidry blotting equipment and stained with Ponceau S. Incubations with monoclonal antibodies or polyclonal antisera were performed by following published protocols (23). Rep and Cap proteins were visualized by alkaline phosphatase-coupled secondary antibodies as described in standard protocols (23) or by peroxidase-coupled secondary antibodies and enhanced chemoluminescence detection (Amersham, Little Chalfont, United Kingdom), as described by the supplier.

For immunoprecipitation experiments, either sucrose gradient fractions from soluble nuclear extracts (500 μl) (67), purified, nonassembled, baculovirus-expressed capsid proteins (14 μl, 100 μg/ml) (60), AAV virus stock (100 μl of 10^9 IU/ml), or purified recombinant VP2/VP3-containing virus-like particles (28 μl, 50 μg/ml) (53) were incubated overnight at 4°C in the presence of 0.5% Nonidet P-40 (NP-40) with 200 μl of hybridoma supernatant of monoclonal antibody A1, A69, B1, or A20 (see below) or 2 μl of a polyclonal capsid protein antiserum raised in a rabbit (VP-S) (53). For control precipitations, we used monoclonal antibody IVA7 (see below), which is directed against the 33-kDa protein of *Onchocerca volvulus*. After this incubation, 2 μl of affinity-purified polyclonal goat anti-mouse immunoglobulins was added to the samples with the monoclonal antibodies as a sandwich for binding to protein A, and the mixtures were incubated for 1 h. To remove nonspecific protein precipitates, the samples were centrifuged for 5 min at 17,600 × g_{av} at 4°C. The immune complexes were precipitated by addition of 30 μl of protein A-Sepharose (10% [wt/vol] in NETN buffer, where NETN buffer consists of 0.1 M NaCl, 1 mM EDTA, 20 mM Tris/HCl [pH 7.5], and 0.5% NP-40). The samples were agitated for 1 h, and the Sepharose beads were washed three times with 1 ml of NETN buffer, boiled in protein-loading buffer, and analyzed by SDS-PAGE and Western blotting. All incubations were done at 4°C. For immunoprecipitation of metabolically labeled proteins, 5×10^5 cells were infected as described above either with AAV-2 and adenovirus type 2 or with adenovirus alone. After 20-h, the cells were incubated for 1 h in DMEM free of methionine and cystine and then for 3 h in the same medium containing 100 μCi of ^{35}S-translabeling mix (ICN Biochemicals). The cells were washed twice with phosphate-buffered saline (PBS; 18 mM Na_2HPO_4, 10 mM KH_2PO_4, 125 mM NaCl [pH 7.2]) and lysed directly in the dish with 1 ml of RIPA buffer (150 mM NaCl, 1% NP-40, 0.5% deoxycholate, 0.1% SDS, 50 mM Tris/HCl [pH 8.0]) for 15 min at 4°C. The lysates were centrifuged for 15 minutes at 17,600 × g_{av} at 4°C, and the supernatants were immunoprecipitated as described above.

Generation of monoclonal antibodies. Monoclonal antibodies against AAV-2 capsid proteins (A1, A69, B1, and A20), replication proteins (76/3), and an adenovirus protein (A30) were generated as described previously (67). The nucleolus-specific antibodies were obtained commercially (Paesel & Lorei, Hanau, Germany), and antibody IVA7, directed against the 33-kDa protein of *O. volvulus*, was kindly provided by R. Lucius, University of Heidelberg.

Immunofluorescent staining. Cells were grown on coverslips and were transfected and infected as described above. Before fixation, the cells were washed for 5 min in PBS and fixed in methanol (5 min at 4°C) and then in acetone (5 min at 4°C). Then the coverslips were air dried and either stored dry at −20°C or used directly for immunofluorescence staining. Alternatively, cells were fixed in 2% paraformaldehyde (PFA) in PBS for 20 min. After incubation in PFA, the coverslips were incubated for 3 min in 50 mM $(NH)_4Cl$ in PBS and for 5 min in 0.5% Triton X-100 in PBS. Then they were washed in PBS. All steps of the PFA fixation were performed at room temperature. PFA-fixed cells were directly used without air drying for immunofluorescence staining. The first antibody was applied to the coverslips for 1 h at 20°C or 15 h at 4°C in a moist chamber. Hybridoma supernatants were applied undiluted, and polyclonal antisera were diluted 1:50 in PBS containing 1% bovine serum albumin (BSA) prior to application. After incubation with the first antibody, the samples were washed three times in PBS for 5 min each at 20°C. The samples were incubated for 1 h at 20°C with either fluorescein- or rhodamine-coupled anti-mouse or anti-rabbit secondary antibodies (Dianova, Hamburg, Germany) diluted 1:50 or 1:100 in PBS–1% BSA. After incubation, the samples were washed as described above and then given short rinses in distilled water and in 100% ethanol. Then the coverslips were air dried, embedded in Elvanol, visualized, and photographed with a Leitz Dialux 22-Microscope, using Kodak T-Max 400 films. For counting fluorescence-positive cells, 5 to 10 randomly chosen image fields each displaying between 100 and 400 cells were evaluated.

Fluorescent in situ hybridization. Coverslips with adherent cells were washed three times in PBS and fixed with 4% PFA in PBS for 20 min. Then the cells were permeabilized by incubation for 20 min in PBS containing 0.5% (vol/vol) Triton X-100 and 0.5% (vol/vol) saponin. After permeabilization, they were washed again in PBS three times, placed in 0.1 M HCl for 5 min, and incubated for 30

minutes at room temperature in PBS containing 20% glycerol. Then the samples were immersed in liquid nitrogen for 2 min and thawed slowly at room temperature. This freeze-thaw step was repeated three times. The coverslips were either stored at −70°C or directly used for in situ hybridization. A *Cla*I-*Bsa*I fragment of pTAV-2 which covers the first 286 nontranscribed nucleotides of AAV was used for in situ hybridization. It was labeled with Bio-16 dCTP (Sigma, Munich, Germany) by using Ready-To-Go DNA-labeling beads (Pharmacia, Uppsala, Sweden) as specified by the manufacturers. The hybridization mixture was prepared by dissolving 36 ng of the labeled fragment and 8 μg of competitor tRNA in 4 μl of formamide per coverslip. The probe was denatured via incubation at 70°C for 10 min and immediately chilled on ice. Then dextran sulfate and 10× SSC (1.5 M NaCl plus 0.15 M sodium citrate [pH 7.0]) were added to final concentrations of 4 ng of labeled probe per ml, 1 μg of tRNA per μl 2× SSC, 10% dextran sulfate, and 50% formamide. Prior to hybridization, the frozen samples were thawed and washed twice with 2× SSC, incubated with 2× SSC (in 50% formamide) at 90°C for 10 min and washed with ice-cold 2× SSC. Then the samples were incubated with the hybridization mixture for 1 h at 37°C in a moist chamber. After hybridization, they were successively washed in 2× SSC (in 50% formamide) for 15 min at 37°C, 2× SSC for 30 min at room temperature, and 1× SSC for 15 min at room temperature. The coverslips were then rinsed in buffer W (20 mM HEPES [pH 7.2], 150 mM KCl, 0.05% Tween 20) and incubated with fluorescein isothiocyanate-coupled ExtrAvidin (Sigma) for 15 h at 4°C (2 μg of ExtrAvidin per ml in 20 mM HEPES [pH 7.2]–250 mM KCl–0.5 mM dithiothreitol–1% BSA). After two washing steps in buffer W (5 min at 20°C each), the samples were immunolabeled for double staining as described above.

Preparation of AAV proteins and particles. Recombinant AAV proteins and VP2/VP3 particles were prepared by infection of SF9 cells with recombinant baculoviruses expressing VP1, VP2, and VP3 (53, 60). For preparation of AAV-2 capsids for electron microscopy, 5×10^7 HeLa cells were transfected with pCMV-VP, infected with adenovirus (MOI = 10), harvested, and sedimented by centrifugation for 5 min at 200 × g_{av} and 4°C. The pellet was resuspended in 50 ml of PBS and centrifuged again for 5 min at 200 × g_{av} and 4°C. The supernatant was discarded, and the pellet was resuspended in 1 ml of PBS containing 1 mM phenylmethylsulfonyl fluoride, 1 μg of pepstatin per ml, and 3 μg of leupeptin per ml and sonified three times for 10 s on ice (Branson sonifier, level 4). The extract was centrifuged (16,500 × g_{av} for 10 min at 4°C), and the pellet was resuspended in 1 ml of digestion buffer (150 mM NaCl, 50 mM Tris/HCl [pH 8.0], 1 mM EDTA, 5 mM $MgCl_2$). DNase and RNase were added to final concentrations of 50 and 25 μg/ml, respectively, and the extracts were incubated for 3 h at 12°C. After digestion, NaCl was added to a final concentration of 0.5 M. Dithiothreitol and EDTA were added to final concentrations of 10 and 2 mM, respectively. Then the samples were sonified again three times for 10 s each and subjected to agitation for 30 min at room temperature. After the agitation, the extracts were centrifuged for 20 min at 3,500 × g_{av} and 4°C. The supernatant was loaded onto a two-step sucrose cushion, with the lower layer consisting of 200 μl of 50% sucrose in TE buffer (10 mM Tris [pH 7.5], 1 mM EDTA) and the upper layer consisting of 200 μl of 30% sucrose in TE, and the extracts were centrifuged for 2.5 h at 42,000 rpm and 4°C in a Beckman TLS55 rotor. The pellet was resuspended in 300 μl of TE buffer with 0.1 M NaCl and incubated at room temperature for 30 min. Then the samples were centrifuged for 1.5 h at 80,000 rpm and 4°C in a Beckman TLA100.3 rotor, and the sediment was resuspended in 200 μl of 0.3 M NaCl in TE buffer and subjected by agitation for 15 h at 4°C. The samples were cleared by centrifugation for 10 min at 16,500 × g_{av} and 4°C, and the supernatant was stained for electron microscopy with 2% uranyl acetate and examined in a Zeiss EM 10 electron microscope.

RESULTS

Characterization of AAV-2 capsid protein antibodies. To study the intracellular localization of AAV-2 capsid proteins in comparison to the localization of Rep proteins and AAV-2 DNA during AAV-2/adenovirus type 2 coinfections, we raised a number of monoclonal antibodies directed against AAV-2 capsid proteins. Western blot analysis of extracts of AAV-2/adenovirus type 2-infected HeLa cells showed that the hybridoma clone A1 produced antibodies which specifically recognize VP1, antibodies of clone A69 recognize VP1 and VP2, and antibodies of clone B1 react with all three capsid proteins (Fig. 1). The immunoreactive polypeptides exactly comigrated with polypeptides detected with a polyclonal capsid protein antiserum (Fig. 1, VP-S) (53). None of the antibodies tested showed cross-reaction with proteins extracted from HeLa cells infected with adenovirus alone under the conditions tested. Antibodies of clone A20 did not react with capsid proteins in Western blot analyses. Based on the overlapping reading frames of VP1, VP2, and VP3 in the AAV-2 cap gene, these findings indicate that A1 detects an epitope within N-terminal

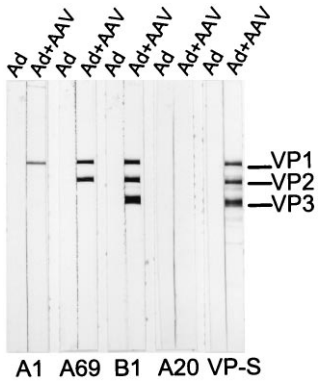

FIG. 1. Immunoblot analysis of monoclonal antibodies raised against AAV capsid proteins. Extracts of HeLa cells infected with adenovirus type 2 (Ad) or AAV-2 plus adenovirus type 2 (AAV+AD) were prepared 24 h postinfection, separated by SDS-PAGE, and blotted. Monoclonal antibodies A1, A69, B1, and A20 were applied to these Western blots and compared with a polyclonal antiserum (VP-S) described previously (53). The antibody reaction was visualized by reaction with an alkaline phosphatase-coupled secondary antibody. Note that A20 does not detect AAV proteins after SDS-PAGE.

amino acids 1 to 137 of VP1, A69 detects an epitope between amino acids 138 and 203 of VP1, corresponding to amino acids 1 to 65 of VP2, and B1 detects an epitope of the VP3 sequence which completely overlaps with VP1 and VP2.

To investigate the specificity of the antibodies toward nondenatured proteins, we immunoprecipitated capsid proteins from extracts of [^{35}S]methionine-labeled HeLa cells infected with AAV-2 and adenovirus type 2 (Fig. 2a) or adenovirus alone (Fig. 2b). Monoclonal antibodies A1, A69, B1, and A20 immunoprecipitated AAV capsid proteins as confirmed by comparison with polypeptides precipitated with the VP-S antiserum. In some precipitations, we recovered a non-AAV-specific polypeptide (Fig. 2a, b, asterisks), but this polypeptide was not specific for a particular antibody and probably represented material nonspecifically adsorbed to protein A-Sepharose. The fact that VP3 was also found in precipitates obtained with antibodies A1 and A69, which do not recognize epitopes of VP3, suggests that VP1 and VP2 are also detected in capsids, capsid precursors, or other complexes involving VP3 (Fig. 2a). To distinguish between these possibilities, we tested the antibodies on more clearly defined substrates, such as recombinant nonassembled capsid proteins purified from baculovirus-infected SF9 cells, assembled capsids present in AAV-2 virus stocks, and recombinant VP2/3 containing empty virus-like particles prepared from baculovirus-infected SF9 cells (Fig. 2c to e). While A1, A69, B1, and VP-S precipitated the recombinant, nonassembled, but partially oligomerized AAV-2 capsid proteins (60), A20 failed to precipitate these proteins, although they were renatured and soluble in buffers of physiological ionic strength (Fig. 2c). A1 and A69 coprecipitated some VP3, probably reflecting complex formation between the capsid proteins. Interestingly, all antibodies except B1 recognized and precipitated capsids from AAV virus stocks (Fig. 2d). Obviously, the epitope which is recognized by B1 becomes masked during capsid assembly. In contrast, A20 antibodies, which failed to detect nonassembled or denatured capsid proteins, precipitated assembled capsids, suggesting that they recognize an epitope which is formed during capsid assembly. These properties of the capsid protein antibodies were confirmed by precipitation of VP2/3 containing virus-like particles (Fig. 2e). In addition it was confirmed that A1 specifically detects VP1, since VP2/3 particles were not precipi-

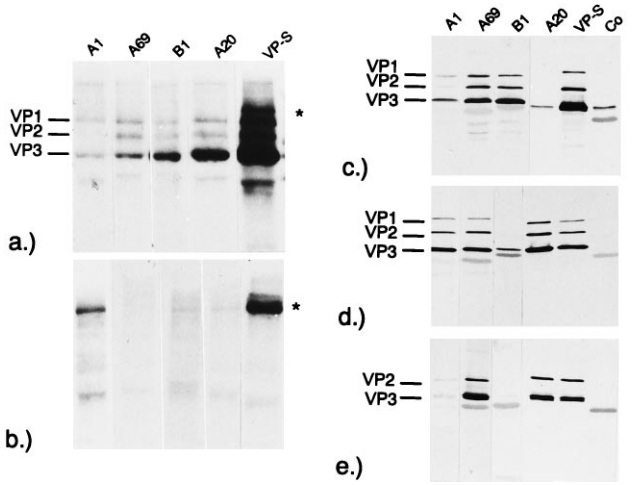

FIG. 2. Immunoprecipitations with monoclonal capsid protein antibodies. (a) Monoclonal antibodies A1, A69, B1, and A20 were used to immunoprecipitate capsid proteins from extracts of [^{35}S]methionine-labeled HeLa cells infected with AAV-2 and adenovirus type 2. (b) Control precipitations were performed with extracts of adenovirus type 2-infected cells. The asterisks denote a nonspecific precipitate in some lanes. (c) Capsid proteins precipitated from a pool of soluble, nonassembled capsid proteins. (d) Capsids precipitated from virus stocks. (e) Precipitation of VP2/VP3 containing capsid-like particles (53). For controls, precipitations with the polyclonal capsid protein antiserum (VP-S) and a nonspecific antibody (Co) were performed. Precipitated capsid proteins were detected by Western blotting with B1 and developing the detected bands with alkaline phosphatase-coupled secondary antibodies.

tated by this antibody. B1 also did not precipitate these virus-like particles. The weakly stained bands migrating below VP3 in Fig. 2c to e are immunoglobulin G molecules of the antibodies. To further clarify the specificity and selectivity of these antibodies for capsid protein populations present in AAV-2/adenovirus type 2-infected HeLa cells, we fractionated nuclear extracts of AAV-2/adenovirus type 2-infected HeLa cells on sucrose gradients and immunoprecipitated the capsid proteins from each fraction (Fig. 3). A1, A69, B1, and VP-S preferentially precipitated VP proteins sedimenting below 20S, representing monomeric or oligomeric capsid proteins. A20 did not precipitate capsid proteins sedimenting in this range. Instead, A20 antibodies selectively precipitated capsid proteins sedimenting around 60S and above (see also reference 67), representing the sedimentation range of empty and full AAV capsids (42). However, it is not clear whether empty and full capsids are recognized with the same affinity. This confirms and extends the conclusion drawn from Fig. 1 and 2 that the A20 antibody specifically recognizes an epitope of assembled capsids which is not present in denatured capsid proteins and native but nonassembled capsid proteins. A1, A69, and VP-S precipitated capsids with lower efficiency than did free capsid proteins. Nevertheless, the specific epitopes for A1, A69, and VP-S are accessible on capsids at least to some extent. Although B1 was highly efficient in precipitating free VP proteins, it precipitated only trace amounts of capsids, which were close to background levels. Taken together with the results of Fig. 2d and e, this antibody can be characterized by a high preference for free capsid proteins; however, a slight reaction with capsids cannot be completely ruled out.

As such, these antibodies, in particular A20 and B1 in combination with polyclonal anticapsid antibodies, e.g., VP-S, are interesting tools for investigating capsid assembly on the cellular level, since they distinguish between free capsid proteins and assembled AAV-2 capsids within infected cells.

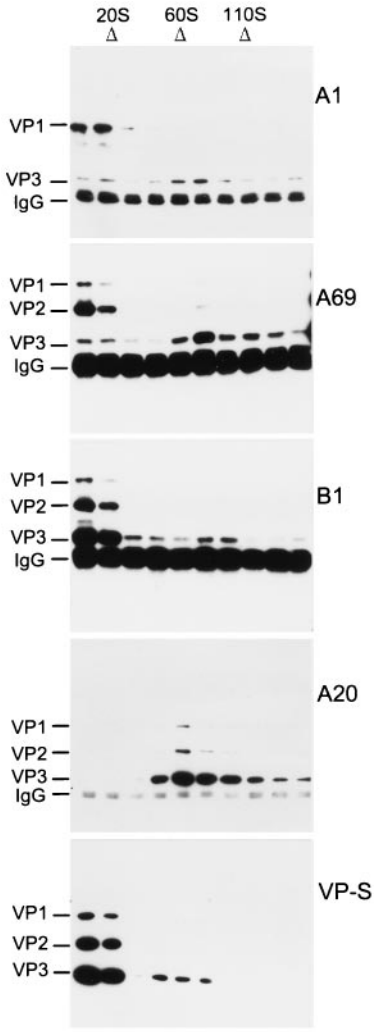

FIG. 3. Immunoprecipitation of size-fractionated capsid proteins obtained from AAV-2/adenovirus type 2-infected HeLa cells with monoclonal capsid protein antibodies. Nuclear extracts of AAV-2/adenovirus type 2-infected HeLa cells were fractionated on sucrose density gradients, and monoclonal antibodies A1, A69, B1, and A20 were used to immunoprecipitate capsid proteins from the fractions obtained. The immunoprecipitates were analyzed by SDS-PAGE and Western blotting with monoclonal antibody B1. The immunoreaction was visualized by incubation with a peroxidase-coupled secondary antibody followed by enhanced chemiluminescence detection. Immunoprecipitations were compared with those obtained by precipitation with a polyclonal capsid protein antiserum (VP-S). Sedimentation positions were determined in parallel gradients with thyroglobulin (20S), empty VP2/3 capsid-like particles (60S), and infectious AAV particles (110S).

Stages of AAV-2/adenovirus type 2 coinfection characterized by the intracellular localization of Rep and Cap proteins. After staining of HeLa cells infected with AAV-2 and adenovirus type 2 (MOI_{AAV} = 20, MOI_{Ad} = 2) by double immunofluorescence with the polyclonal antiserum VP-S, recognizing all capsid proteins, and monoclonal antibody 76-3, recognizing the nonspliced Rep proteins Rep78 and Rep52 (67), we observed a number of different phenotypes regarding the spatial intracellular distribution of Rep and Cap proteins. We classified them into five groups defined by typical patterns of intracellular Rep and Cap protein distribution (Fig. 4a) and counted their frequencies at consecutive time points after infection. As shown in Fig. 4b, different phenotypes, defined as stages 2 to 5, exhibited their peaks of relative frequency at

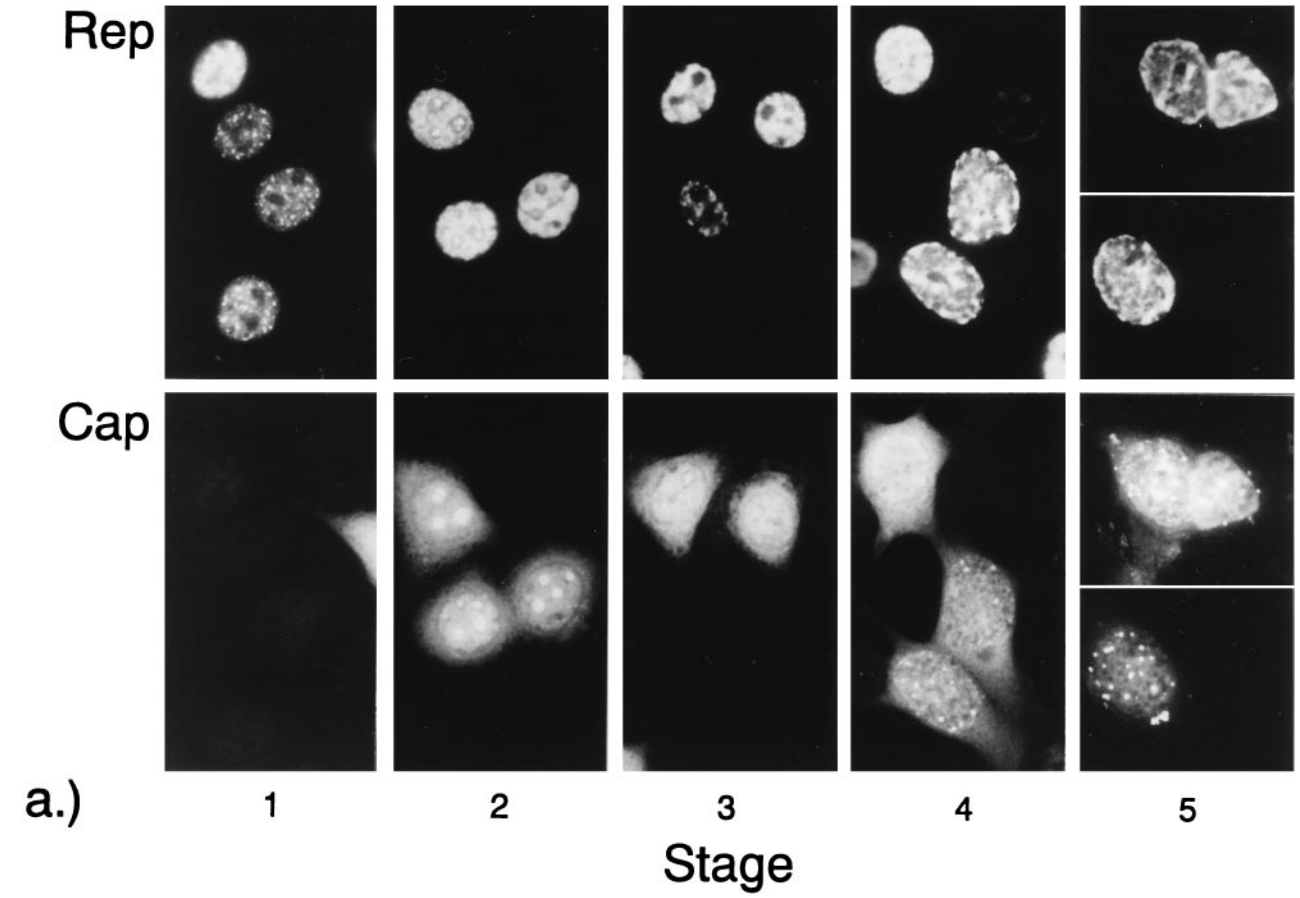

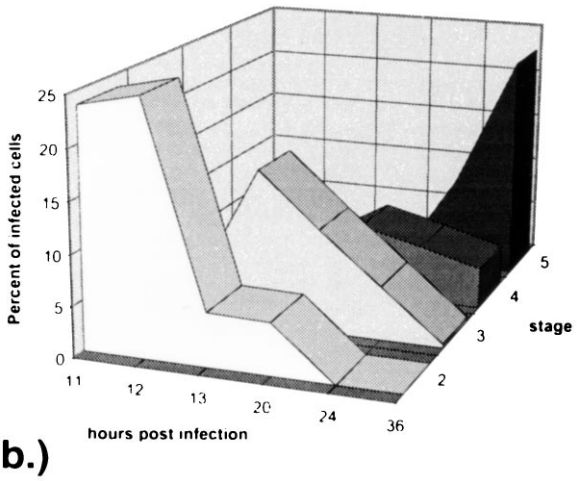

FIG. 4. Characterization of stages of a productive AAV-2/adenovirus type 2 coinfection in HeLa cells by double immunofluorescence with Rep and Cap antibodies. (a) The subcellular localization of replication proteins (Rep) and capsid proteins (Cap) was visualized with the polyclonal VP antiserum and monoclonal antibody 76/3, recognizing Rep78 and Rep52 (67), in samples prepared during the time course of infection by double immunofluorescence staining. (b) The succession of five stages shown in panel a was analyzed by determining the frequency of defined subcellular Rep and Cap distributions in a population of coinfected cells at various time points postinfection. Stage 1 was omitted from the graph, since its frequency remained constant throughout the infection, although it appeared before the other stages.

different time points postinfection. This allowed us to postulate a sequence of stages representing the progression of an AAV-2/adenovirus type 2 coinfection.

Stage 1 clearly appeared at earlier time points than stage 2, between 10 and 14 h after infection, but did not decline in frequency when the following stages appeared. This made it difficult to include the frequency distribution of stage 1 in the graph shown in Fig. 4b. Between 70 and 80% of the cells showed this distribution of the Rep proteins. The observation that a higher proportion of cells, up to 90% and more, appeared in stages 2 to 5 when the MOI of adenovirus was enhanced suggests that at low MOI of adenovirus relative to the MOI of AAV-2 there is a block of progression to the following stages in some cells (data not shown). The dotted distribution pattern of Rep proteins probably represents sites of AAV DNA replication (65), since AAV-2 DNA colocalized in the same spots (see Fig. 7). At this stage, no capsid proteins which could be used for packaging of the replicated DNA were expressed, whereas cells in stage 2 expressed both Rep and Cap proteins. In stage 2, Rep proteins were detectable all over the nucleoplasm and occasionally were also visible in the nucleoli as a group of small fluorescence-positive clusters. We interpret this as a short transient nucleolar state of Rep (e.g., Fig. 4, stage 2), since Rep was not detectable in nucleoli in the preceding or following stages. Capsid proteins were detectable in the nucleus and in the cytoplasm and were clearly enriched in the nucleoli. The identity of the nucleoli was confirmed with a commercially available nucleolus specific antibody (data not shown). In stage 3, large amounts of Rep and capsid proteins

were present in the nucleoplasm; however, capsid proteins were also detectable in the cytoplasm and the nucleoli. The nucleoli, if detectable, were strongly enlarged or fragmented and began to disappear. In this stage, the most extensive colocalization of replication and capsid proteins in broad zones of the nucleoplasm was observed. The colocalization of Rep and Cap proteins of some of the samples shown here by conventional immunofluorescence microscopy was verified by laser scanning microscopy of doubly stained samples (data not shown). In stages 4 and 5, Rep proteins concentrated in some clusters of the nucleus, often along the nuclear periphery, and the capsid proteins were no longer codistributed in these stages. Some of these redistributions might be due to adenovirus-induced changes of the nuclear structure. Furthermore, an increasing amount of strongly capsid protein-positive dots became visible both in the nucleus and in the cytoplasm. These stages describe the most frequent images and omit intermediates and rare patterns of Rep and Cap distribution. The localization pattern of replication and capsid proteins was confirmed after fixation of cells with PFA (data not shown).

VP1 and VP2 accumulate in the nucleus, in contrast to VP3. Comparison of the distribution patterns of VP1 alone (determined by antibody A1), VP1 plus VP2 (determined by antibody A69), and nonassembled VP1 plus VP2 plus VP3 (determined by antibody B1) with those of total capsid proteins (detected by the VP-S serum) showed some interesting details (Fig. 5). VP1 and VP2 were highly enriched in the nucleus, while nonassembled VP3 detected with B1 was evenly distributed over the nucleus and cytoplasm. This result suggests that the stoichiometry of capsid proteins is different in the nuclear and cytoplasmic compartments. As B1, in contrast to VP-S, does not detect assembled capsids, it seems likely that the higher proportion of the VP-S-positive material in the nucleoplasm accounts for assembled capsids. All three monoclonal antibodies, A1, A69, and B1, showed similar rearrangements of nuclear compartmentalization of capsid proteins during the time course of infection, as shown in Fig. 4 with the VP antiserum (data not shown).

Localization of AAV-2 capsids during the time course of infection. To localize the cellular compartment of capsid formation, we used the capsid-specific antibody A20 in double-immunofluorescence stainings with the polyclonal capsid protein antiserum (VP-S) to visualize AAV-2 capsids in AAV-2/adenovirus type 2-coinfected HeLa cells at various time points postinfection. Between 10 and 14 h after infection (transition of stage 1 to stage 2), VP proteins were distributed over the cytoplasm and the nucleoplasm while the nucleoli were negative. At this time, no AAV-2 capsids were detectable (Fig. 6a). Before 10 h postinfection, no immunofluorescence was seen, demonstrating that the VP-S antiserum detected newly synthesized capsid proteins. At later time points (stage 2 and the transition between stage 2 and stage 3), capsid proteins accumulated in the nucleoli, which increased in size and intensity of staining for capsid proteins (Fig. 6b to d). Coincidentally with the nucleolar localization of capsid proteins, AAV-2 capsids were detectable with the A20 antibody. Counting the frequencies of various A20-positive images at early time points after infection suggested that the nucleoli were the sites in infected cells where capsids were first detected (Fig. 6i), although at the earliest stages a significant number of cells also showed some nucleoplasmic staining. The nucleoli gradually increased in size during infection (Fig. 6b to d) and finally seemed to become fragmented (Fig. 6e) or completely dissolved (Fig. 6f). At intermediate stages (stage 3 and 4), capsids colocalized with capsid proteins in the nucleoli and the nucleoplasm; however, they were never detectable in the cytoplasm at these stages

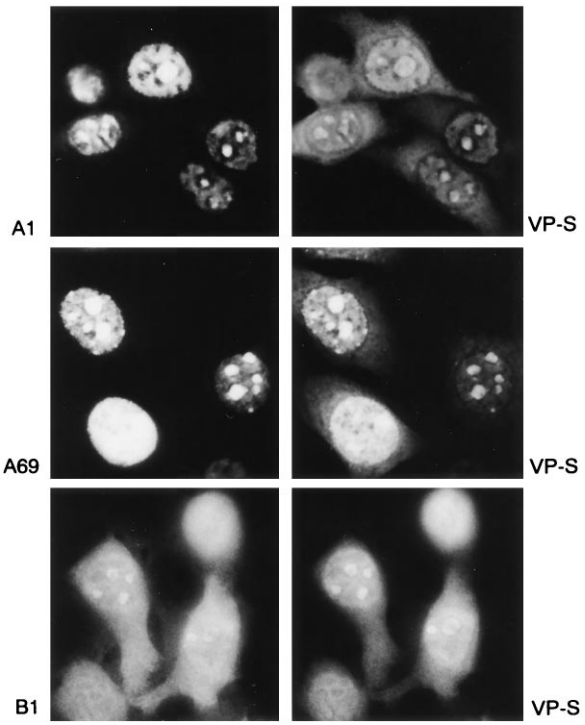

FIG. 5. Subcellular localization of VP1, VP1/2, or VP1/2/3 in AAV-2/adenovirus type 2-infected HeLa cells. Double immunofluorescence with monoclonal antibodies A1, A69, B1, and the VP antiserum (VP-S) at stages 2 to 3 is shown. B1 (reacting with VP1, VP2 and VP3) detected nuclear and cytoplasmic capsid proteins with similar intensity, whereas A1 (reacting with VP1) and A69 (reacting with VP1 and VP2) exclusively stained nuclear capsid proteins.

(Fig. 6d to f). Only very late in the progression of the infection were capsids released to the cytoplasm. They did not colocalize with the bulk of capsid proteins (Fig. 6g and h). These results clearly indicate that capsid assembly is confined to nuclei of infected cells and that the nucleoli or nucleolar components may play a role in the assembly process.

Localization of AAV-2 DNA in relation to Rep and Cap proteins. To define potential sites for AAV DNA packaging, we performed fluorescent in situ hybridization experiments in combination with immunofluorescent stainings to compare the distribution patterns of Rep and Cap proteins with the localization of AAV-2 DNA (Fig. 7). In cells of stage 1, Rep and AAV-2 DNA colocalized in the finely dotted pattern already described for Rep localization in Fig. 4, an observation which recently was also made by others (65). As mentioned above, capsid proteins were not detectable at this stage. In stages 2 and 3, Rep and DNA still colocalized over large areas of the nucleoplasm and weak signals inside the nucleoli could sometimes be observed. During these stages, localization of the capsid proteins visualized with the B1 antibody overlapped with DNA in the nucleoplasmic areas, but DNA was either absent from the nucleoli or present in only very small amounts, although the nucleoli were the sites of strongest capsid protein fluorescence. Double staining of AAV DNA and capsids with the capsid-recognizing antibody (A20) was not successful because a denaturation step was necessary for DNA hybridization and the A20 antibodies did not react with denatured capsid proteins. We were unable to detect AAV-2 DNA in cells harvested 30 h postinfection (stages 4 and 5 [data not shown]), suggesting that the amount of DNA accessible for hybridization was too small at late stages of infection because

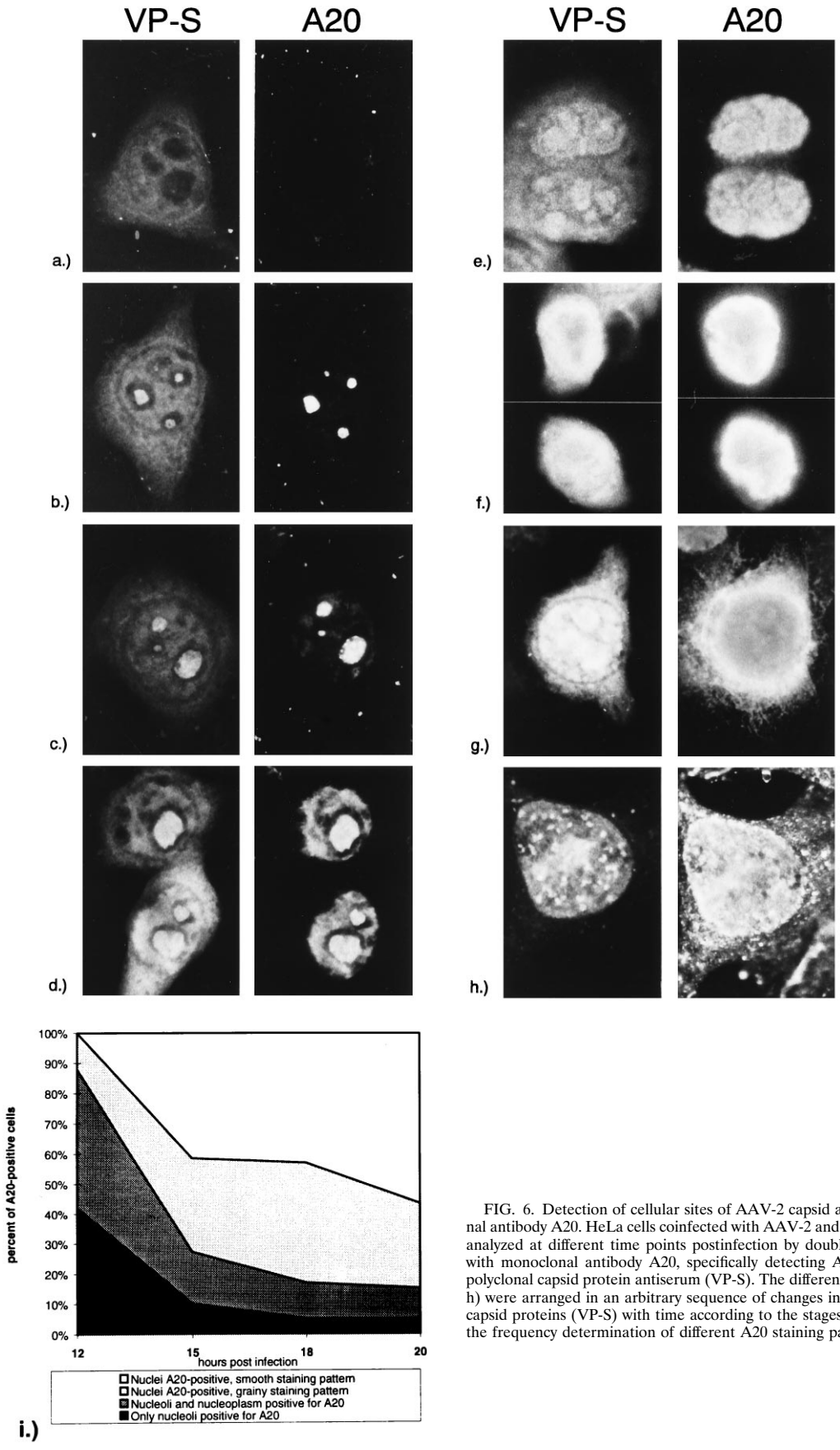

FIG. 6. Detection of cellular sites of AAV-2 capsid assembly with monoclonal antibody A20. HeLa cells coinfected with AAV-2 and adenovirus type 2 were analyzed at different time points postinfection by double immunofluorescence with monoclonal antibody A20, specifically detecting AAV-2 capsids and the polyclonal capsid protein antiserum (VP-S). The different staining patterns (a to h) were arranged in an arbitrary sequence of changes in cellular localization of capsid proteins (VP-S) with time according to the stages depicted in Fig. 4 and the frequency determination of different A20 staining patterns (i).

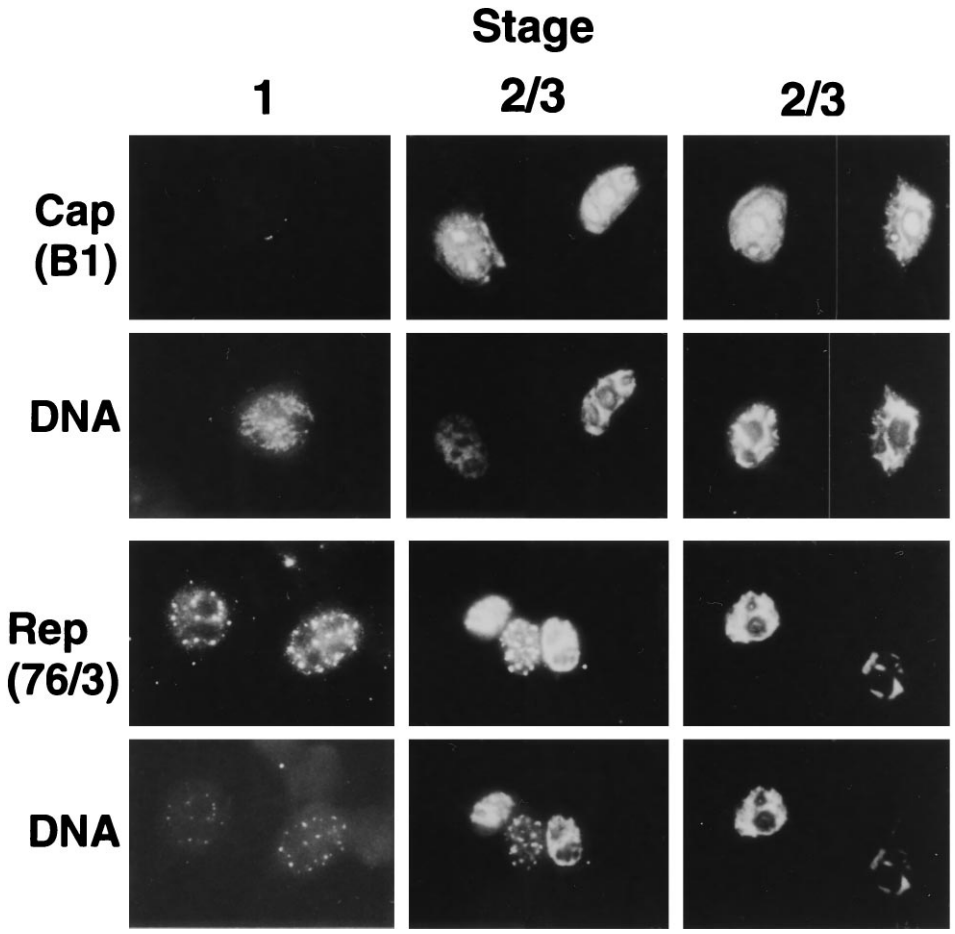

FIG. 7. Subcellular localization of AAV-2 DNA in comparison to Rep and Cap proteins in AAV-2/adenovirus type 2-infected HeLa cells. Double staining of AAV-2/adenovirus type 2-coinfected HeLa cells was performed using indirect immunofluorescence and in situ hybridization techniques. The localization of AAV-2 DNA was shown in comparison to capsid proteins by detection with monoclonal antibody B1 and in comparison to the nonspliced Rep proteins visualized with monoclonal antibody 76/3 for stage 1 and stages 2 and 3 of an AAV-2/adenovirus type 2 coinfection. Note the complete colocalization of AAV-2 DNA and Rep proteins and the only partial colocalization of AAV-2 DNA and capsid proteins in the nuclei of infected cells.

most of the AAV-2 DNA had already been packaged. As such, the nucleoplasm is an area where replication proteins, capsid proteins, and DNA colocalize and where DNA packaging might occur.

Genetic elements of AAV-2 involved in capsid formation. Detection of capsids by the A20 antibody allowed us to investigate which AAV-2 genes are involved in capsid formation. HeLa cells were transiently transfected with a plasmid containing the complete AAV genome (pTAV-2) and infected with adenovirus, and capsid formation was monitored by A20 immunofluorescence in comparison to cells transfected with a construct expressing the cap gene alone (pCMV-VP) (Fig. 8). Transfection of pTAV-2 and infection with adenovirus led to the formation of capsids in about 90% of capsid protein-expressing cells (equivalent to AAV-2/adenovirus type 2-coinfected cells), and the cells proceeded through the same stages as in a coinfection experiment (data not shown). Only the cells showing nucleolus-localized capsid proteins also showed capsid formation (Fig. 8a, pTAV-2). This correlation also held true for cells expressing solely the cap gene, regardless of whether they were infected with adenovirus (Fig. 8a, pCMV-VP +Ad, pCMV-VP −Ad). Preparative isolation of capsids from such transfected cells and analysis by negative staining and electron microscopy confirmed that capsids were indeed assembled (data not shown). However, two differences were obvious when cells transfected with pCMV-VP were compared with cells transfected with pTAV-2: first, the capsids accumulated in the enlarged nucleoli and did not proceed through the following stages of infection, and second, only about 40% of the capsid protein-expressing cells also formed capsids as quantitated by comparison of VP-S- and A20-positive cells. Therefore, we tried to determine which components of the AAV genome enhance the efficiency of capsid formation and which factors have an influence on the subcellular distribution of capsids.

Transfection of increasing amounts of the AAV cap gene expression plasmids (CMV-VP) resulted in a nearly exponential increase in the percentage of capsid-producing cells (Fig. 8b), showing that capsid formation is strongly dependent on cellular capsid protein concentration.

When we studied the influence of different Rep proteins or of replication-competent plasmids with terminal repeats on the efficiency of capsid formation, we were not able to detect a direct and reproducible stimulation of capsid assembly by these components (data not shown). An indirect effect due to changes of the intracellular capsid protein concentration could not be excluded. However, when we analyzed the subcellular distribution of capsids, we observed an altered pattern of cap-

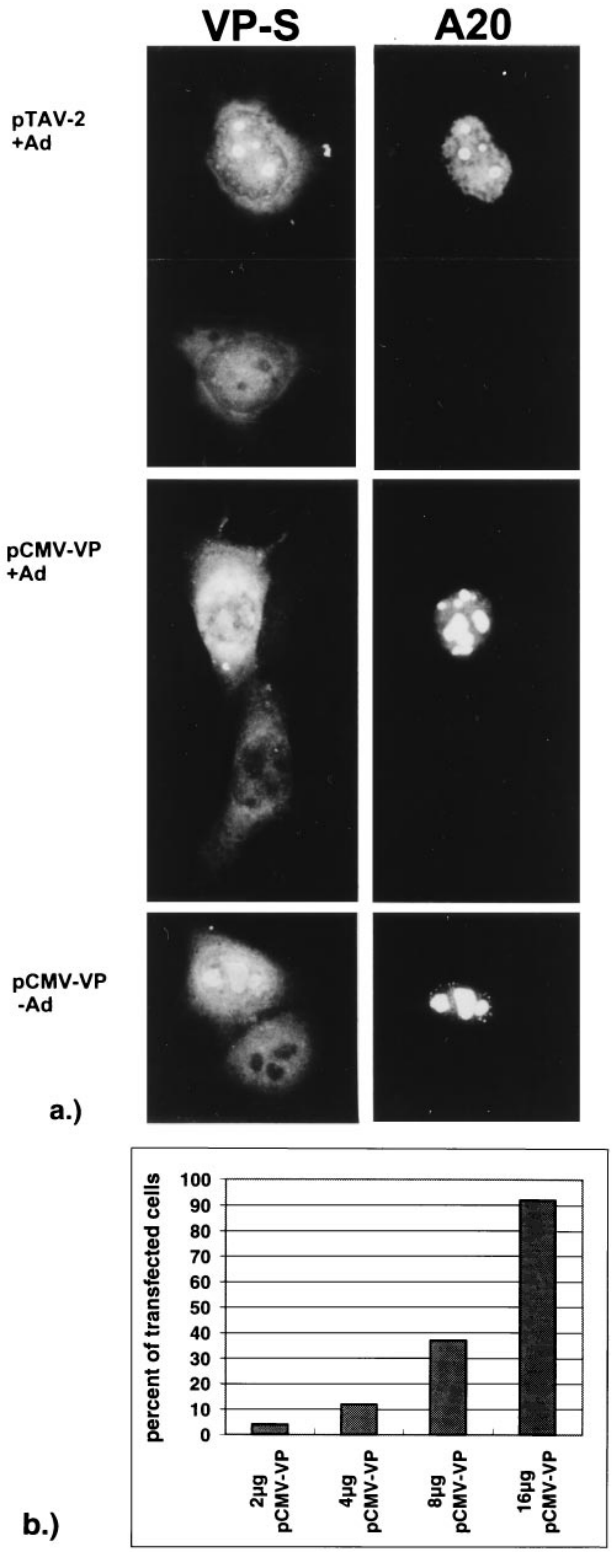

FIG. 8. Capsid assembly in HeLa cells transfected with a full-length AAV-2 genome or the cap gene alone. (a) HeLa cells were transfected with plasmids containing a full-length AAV-2 genome (pTAV-2) or the cap gene expressed under the control of the CMV promoter (CMV-VP) in the presence or absence of adenovirus type 2 (Ad) and analyzed for capsid formation by double immunofluorescence with the polyclonal capsid protein antiserum (VP-S) and monoclonal antibody A20 for detection of capsid formation. (b) The percentage of capsid protein-expressing cells which formed capsids was determined by the same assay after transfection of increasing quantities of CMV-VP plasmid.

sid distribution when Rep proteins were coexpressed (Fig. 9). As mentioned above, expression of the cap gene alone led to the formation of capsids which were restricted to the nucleoli, in contrast to the accumulation of capsids throughout the nucleoplasm in the presence of the whole AAV genome (Fig. 9, pTAV2 and pCMV-VP + pKEX). Coexpression of the small Rep proteins in most cells resulted in a punctate distribution pattern of assembled capsids (Fig. 9). This was accompanied by a significantly reduced capsid protein expression level and reduced capsid formation efficiency (data not shown). Coexpression of Rep78 or Rep 68 seemed to permit the release of assembled capsids from the nucleoli or stimulated capsid assembly outside the nucleoli also, leading to a capsid distribution rather similar to the situation in AAV-2/adenovirus type 2-coinfected cells (Fig. 9). This effect was capsid protein concentration independent, and cotransfection of a plasmid with AAV terminal repeats did not change this pattern. This result clearly showed an influence of the Rep proteins on the subcellular distribution of assembled AAV capsids.

DISCUSSION

Analysis of cellular compartmentalization of AAV-2 DNA, Rep, and Cap proteins during the course of a productive infection provided evidence for temporal and spatial regulations of DNA replication, capsid assembly, and DNA packaging. The whole process could be described in a number of characteristic stages of infection. The spatial distribution of capsid protein subgroups, including the distribution of assembled and nonassembled capsid proteins by specific monoclonal antibodies, allowed us to determine the cellular sites of capsid assembly and packaging and finally to identify AAV genes involved in capsid assembly and localization. These data provide a framework for the interpretation of biochemical and genetic data describing the process of AAV reproduction.

An important tool for the analysis of subcellular capsid protein localization was a set of monoclonal antibodies which allowed us to distinguish between proteins VP1 (A1), VP1 plus VP2 (A69), and VP1 plus VP2 plus VP3 (B1) and between nonassembled capsid proteins (B1) and assembled capsids (A20). The specificity of these antibodies was established by Western blotting and immunoprecipitations with a number of different substrates. Only the A1 antibody occasionally reacted with a non-AAV-derived protein in immunoprecipitations, whereas the other antibodies showed cross-reactions only at very high concentrations of antibodies and protein and after prolonged exposure. The cross-reaction of A1 was variable and of low affinity compared to the reaction with the VP1 polypeptide, since, for example is was not detectable when VP1 was precipitated from extracts of AAV-2/adenovirus type 2-infected HeLa cells. Immunoprecipitations with the VP1- or VP1/VP2-specific antibodies A1 and A69, respectively, resulted in a weak precipitation not only of assembled capsids but also of nonassembled VP3, suggesting that the epitopes for VP1 and VP2 are accessible both in assembled capsids and in nonassembled capsid precursor complexes containing VP1 and VP3. In contrast, the antibody reacting with all three capsid proteins (B1) did not significantly precipitate assembled capsids according to several criteria. It is more difficult to interpret the characteristics of the A20 antibody. This antibody certainly has a high affinity for assembled capsids, and the Western blotting and immunoprecipitation experiments suggest that it recognizes a conformational epitope which is absent in denatured or nonassembled native capsid protein. The epitope is also present in recombinant virus-like particles made up of VP2 and VP3. It is, however, difficult to exclude the possibility

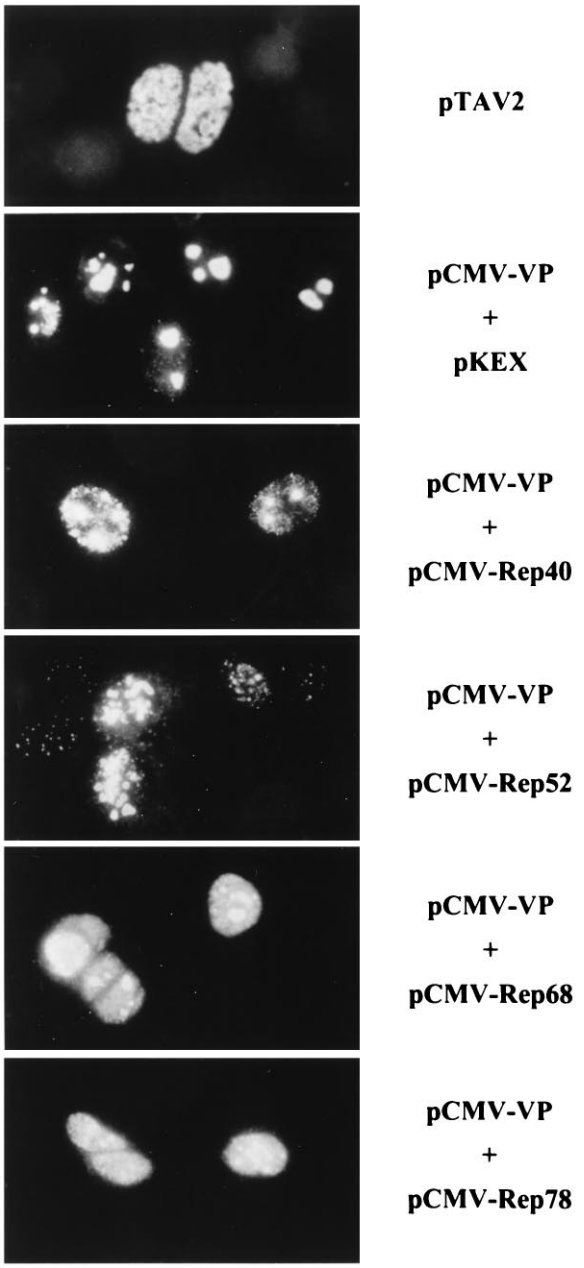

FIG. 9. Rep proteins influence the subcellular distribution of assembled AAV capsids. HeLa cells were transfected with a plasmid containing the complete AAV genome (pTAV-2) or the AAV-2 cap gene alone (pCMV-VP) or the cap gene in combination with single Rep protein expression constructs (pCMV-Rep40, pCMV-Rep52, pCMV-Rep68, and pCMV-Rep78) and infected with adenovirus type 2 18 h after transfection. Cells were fixed 20 h after infection and stained with monoclonal antibody A20 to detect AAV-2 capsids. Note the different subcellular distribution patterns of AAV capsids.

that this antibody also reacts with capsid precursors which possibly already have acquired the specific conformational epitope. Keeping this precaution in mind, this antibody is a very useful tool for the analysis of the AAV assembly process.

The immunofluorescence data obtained with the A20 antibody clearly showed that capsid assembly is a nuclear process. The antibody characteristics of A1 and A69 allowed us to show that VP1 and VP2, unassembled and assembled, are highly enriched in the nucleus whereas unassembled VP3 is equally distributed between both compartments or somewhat enriched in the cytoplasm. This observation already implies that the stoichiometry of VP1 and VP2 to VP3 must be different in the nucleus and in the cytoplasm. This conclusion seems to contradict the analysis of capsid proteins obtained by preparation of nuclear and cytoplasmic fractions of infected cells (67). Such fractionation data, however, often lead to a mislocalization of highly soluble proteins, such as, e.g., the small Rep proteins, due to the leakiness of prepared nuclei. Expression of single capsid proteins also showed that VP1 and VP2 efficiently entered the nucleus whereas VP3 only equilibrated between both compartments (53). Coexpression of VP1 or VP2 with VP3 increased the nuclear accumulation of VP3, suggesting that VP1 and VP2 are able to cotransport VP3 to the nucleus as has also been shown for capsid proteins of other viruses (30). Such a heterotypic complex formation for nuclear transport of a particular capsid constituent could be a mechanism to enrich the capsid proteins in the correct stoichiometry for capsid assembly in the nucleus. Assembly experiments with single capsid proteins expressed by infections with recombinant baculoviruses are in line with these speculations, since capsid-like structures could be detected in VP3-expressing SF9 cells only when VP2 was coexpressed (53). Recently, the expression of single capsid proteins in HeLa cells also showed that VP3 alone was incapable of assembling into capsids as analyzed by immunofluorescence with the A20 antibody (60).

Strikingly, the capsid proteins accumulated in the nucleoli of HeLa cells in early stages of infection or when expressed by transfection of the cap gene. We observed capsid formation only in cells in which the capsid proteins had entered the nucleoli. Exceptions were cells in which nucleoli could no longer be detected, either due to progression of the infection or to the disassembly of the nucleoli during the cell cycle (e.g., Fig. 6e to h). Cells which expressed the capsid proteins but in which the nucleoli were clearly capsid protein negative never showed any signs of capsid formation. This suggests that nucleolar components are involved in the capsid assembly process. In kinetic studies, capsids clearly were first detected in the nucleoli of a large proportion of infected cells; however, at the same time, smaller amounts of capsids in addition to the ones localized in the nucleoli were also detectable at some nucleoplasmic sites in a similar proportion of infected cells. Since A20 fluorescence is an indicator for capsids but not for the assembly process itself and the capsid localization pattern changes with time, this could reflect capsids which had already been released or exported from the nucleoli. Alternatively, initiation of capsid assembly could also occur at these nucleoplasmic positions. The transfection studies support the first interpretation, since in the presence of the cap gene alone, capsids were detectable almost exclusively in highly enlarged nucleoli. The fact that coexpression of the large Rep proteins leads to a significant increase of extranucleolar capsids can be interpreted as an influence of the Rep proteins on relocalization of the assembled capsids from the nucleoli to the nucleoplasm. The alternative interpretation, i.e., that Rep stimulates capsid assembly outside the nucleoli, possibly by recruitment of assembly factors at these sites, cannot be excluded. Although the presented data do not allow us to postulate an assembly pathway which obligatorily goes through the nucleolus in infected cells, the nucleolar localization of capsids during AAV infection is strikingly prominent. A high concentration of empty parvovirus H-1 particles in the nucleolus was also observed in early electron microscopic studies (1, 56). Capsid assembly undoubtedly depends on the capsid protein concentration, and since capsid proteins accumulate in the nucleoli, they might represent just the cellular sites where the critical concentration for capsid

assembly is first reached. This simple interpretation, however, is questionable, since capsid proteins did not continuously concentrate in the nucleolus. In transfection and infection experiments, one could observe many cells which showed a strong capsid protein fluorescence while the nucleoli were empty of capsid proteins, giving the impression that a switch for nucleolar uptake of VP proteins had not yet occurred. The nucleoli are the cellular sites of ribosome biogenesis and harbor many proteins involved in assembly processes. It is therefore tempting to speculate that nucleolar chaperones may also be used for AAV capsid assembly.

According to the model of AAV packaging established by Myers and Carter (42), ssDNA resulting from displacement synthesis is introduced into preformed empty AAV capsids. Genetic evidence showed that in addition to the capsid proteins (25), Rep40 and Rep52 significantly stimulated ssDNA accumulation (17). This means that during AAV-2 DNA packaging, colocalization of Rep proteins, DNA, and capsids should be expected. Rep proteins 78 and 52 and AAV-2 DNA showed a perfect colocalization pattern (see also reference 65). A direct comparison of the localization of capsids and DNA was not possible because denaturation steps required for in situ hybridization of the DNA destroyed the epitope recognized by the A20 antibody. However, comparison of the localization of free capsid proteins by the B1 antibody with AAV-2 DNA and correlation of B1 fluorescence and A20 fluorescence by comparison of the fluorescence obtained with the VP-S antiserum clearly demonstrate that the predominant sites of capsid and DNA colocalization are nucleoplasmic areas at a certain distance from the nucleolus. This means that at the site of the highest capsid concentration and probably the most intensive capsid production, namely, the nucleolus, little or no DNA packaging occurs. Only trace amounts of AAV-2 DNA were detectable in the nucleolus, in contrast to reports of nucleolar localization of minute virus of mice DNA in mouse cells (22, 64). Coinfection with adenovirus also redirected minute virus of mice DNA to multiple intranuclear foci in HeLa cells, similar to the distribution of AAV-2 DNA. Ultrastructural studies of the autonomous H-1 parvovirus replication suggest that DNA synthesis begins at clusters of fibrillar centers released from nucleoli (55), suggesting that destruction of the nucleolus is part of the viral replication and asembly process. This view urges the interpretation that the assembled capsids are released from the nucleoli to the sites of DNA packaging, possible with the aid of the large Rep proteins in the course of nucleolar destruction. Hunter and Samulski (28) observed that AAV Rep and capsid proteins colocalize in the nuclei of infected cells. However, they also observed densely fluorescent capsid regions where they did not see an increase in Rep fluorescence. These regions may correspond to the nucleoli. It is not clear why these authors found a colocalization of Rep and Cap proteins in the foci where Rep proteins and AAV-2 DNA already colocalized, i.e., at a stage when we could not detect capsid protein expression. In the course of the present experiments, colocalization of Rep and capsid proteins could be observed only at stage 2, with a peak at stage 3 when Rep was already distributed in rather broad areas of the nucleoplasm. One possibility is that infections with a higher MOI of adenovirus led to an earlier onset of capsid protein expression than was observed in this study, which could result in an overlap of Rep and Cap localization at an earlier stage of infection than reported here. A close spatial association of replication proteins and DNA but a rather distinct localization of the capsid proteins was also observed for the Aleutian mink disease virus (45), although at different nuclear sites from those observed in this study. The segregation of replicating DNA and replication proteins from capsid proteins and capsids at certain time points postinfection to separate compartments might reflect necessary regulatory events in DNA replication and packaging.

The interpretation of different localization patterns as a process is difficult, because several different images can be observed at a certain time point after infection, and often the tools for revealing the underlying processes are not available. The five stages described above are more or less arbitrarily defined and omit rare images which could not be arranged into an order of events. Several studies have interpreted the distribution pattern of Rep proteins and DNA in a number of foci typically observed in stage 1 as replication centers which increase in size with the duration of infection (28, 65; see above). The strong nucleolar accumulation of capsid proteins in stage 2 could be interpreted as an expression of an intense capsid assembly activity. The nucleoli also increase in size during infection, and capsids finally spread over the nuclear interior, possibly indicating relocation of capsids for packaging. The broad nucleoplasmic zones outside the nucleoli and not directly associated with the nuclear envelope harboring AAV DNA, Rep proteins, and capsid proteins are probably the areas of DNA packaging. They are formed in stage 2 and 3 and last for about 2 h. Interpretation of clusters of Rep proteins or the speckles of capsid proteins where no capsids are detectable at later stages (stages 4 and 5) is not possible at present. The fine network of capsid fluorescence emerging from the nuclei of AAV-producing cells which often ends at the surface of not yet infected cells might depict the path of virion release and attachment at cells for a new round of infection.

ACKNOWLEDGMENTS

A. Wistuba is supported by a fellowship of the German-Israeli Cooperation in Cancer Research.

We are grateful to B. Hub and U. Ackermann for expert technical assistance in electron microscopy and photography. We thank H. zur Hausen for continuous support and M. Pawlita and H. Zentgraf for critical reading of the manuscript.

REFERENCES

1. **Al-Lami, F., N. Ledinko, and H. Toolan.** 1969. Electron microscope study of human NB and SMH cells infected with the parvovirus, H-1: involvement of the nucleolus. J. Gen. Virol. **5:**485–492.
2. **Ashktorab, H., and A. Srivastava.** 1989. Identification of nuclear proteins that specifically interact with adeno-associated virus type 2 inverted terminal repeat hairpin DNA. J. Virol. **63:**3034–3039.
3. **Atchinson, R. W., B. C. Castro, and W. M. Hammon.** 1965. Adeno-associated defective particles. Science **149:**754–756.
4. **Baines, J. D., R. J. Jacob, L. Simmermann, and B. Roizman.** 1995. The herpes simplex virus 1 UL11 proteins are associated with cytoplasmic and nuclear membranes and with nuclear bodies of infected cells. J. Virol. **69:** 825–833.
5. **Beaton, A., P. Palumbo, and K. I. Berns.** 1989. Expression from the adeno-associated virus p5 and p19 promoters is negatively regulated in *trans* by the rep protein. J. Virol. **63:**4450–4454.
6. **Berezney, R.** 1991. The nuclear matrix: a heuristic model for investigating genomic organization and function in the cell nucleus. J. Cell. Biochem. **47:**109–123.
7. **Berns, K. I.** 1990. Parvovirus replication. Microbiol. Rev. **54:**316–329.
8. **Berns, K. I., and R. A. Bohenzky.** 1987. Adeno-associated viruses: an update. Adv. Virus Res. **32:**243–306.
9. **Bosher, J., A. Dawson, and R. T. Hay.** 1992. Nuclear factor I is specifically targeted to discrete subnuclear sites in adenovirus type 2-infected cells. J. Virol. **66:**3140–3150.
10. **Bridge, E., D. X. Xia, M. Carmo-Fonseca, B. Cardinali, A. I. Lamond, and U. Pettersson.** 1995. Dynamic organization of splicing factors in adenovirus-infected cells. J. Virol. **69:**281–290.
11. **Buller, R. M. L., J. Janik, E. D. Sebring, and J. A. Rose.** 1981. Herpes simplex virus types 1 and 2 completely help adeno-associated virus replication. J. Virol. **40:**241–247.

12. **Carter, B. J.** 1990. Adeno-associated virus helper functions, p. 255–282. *In* P. Tijssen (ed.), Handbook of parvoviruses. CRC Press, Inc., Boca Raton, Fla.
13. **Carter, K. C., D. Bowman, W. Carrington, K. Fogarty, J. A. McNeil, F. S. Fay, and J. B. Lawrence.** 1993. A Three-dimensional view of precursor messenger RNA metabolism within the mammalian nucleus. Science **259:** 1330–1335.
14. **Carvalho, T., J. S. Seeler, K. Ohman, P. Jordan, U. Pettersson, G. Akusjarvi, M. Carmo-Fonseca, and A. Dejean.** 1995. Targeting of adenovirus E1Aand E4-ORF3 proteins to nuclear matrix-associated PML bodies. J. Cell Biol. **131:**45–56.
15. **Chang, L. S., and T. Shenk.** 1990. The adenovirus DNA-binding protein stimulates the rate of transcription directed by adenovirus and adeno-associated virus promoters. J. Virol. **64:**2103–2109.
16. **Chang, L. S., Y. Shi, and T. Shenk.** 1989. Adeno-associated virus p5 promoter contains an adenovirus E1A-inducible element and a binding site for the major late transcription factor. J. Virol. **63:**3479–3488.
17. **Chejanovsky, N., and B. J. Carter.** 1989. Mutagenesis of an AUG codon in the adeno-associated virus rep gene: effects on viral DNA replication. Virology **173:**120–128.
18. **Chen, C., and H. Okayama.** 1987. High-efficiency transformation of mammalian cells by plasmid DNA. Mol. Cell. Biol. **7:**2745–2752.
19. **DeBruyn Kops, A., and D. M. Knipe.** 1988. Formation of DNA replication structures in herpes virus-infected cells requires a viral DNA binding protein. Cell **55:**857–868.
20. **DeBruyn Kops, A., and D. M. Knipe.** 1994. Preexisting nuclear architecture defines the intranuclear location of herpesvirus DNA replication structures. J. Virol. **68:**3512–3526.
21. **DeWet, J. R., K. V. Wood, M. DeLuca, D. R. Helinski, and S. Subramani.** 1987. Firefly luciferase gene: structure and expression in mammalian cells. Mol. Cell. Biol. **7:**725–737.
22. **Fox, E., P. T. Moen, Jr., and J. W. Bodnar.** 1990. Replication of minute virus of mice DNA in adenovirus-infected or adenovirus-transformed cells. Virology **176:**403–412.
23. **Harlow, E., and D. Lane.** 1988. Antibodies: a laboratory manual. Cold Spring Harbor Laboratory, Cold Spring Harbor, N.Y.
24. **Heilbronn, R., A. Bürkle, S. Stephan, and H. zur-Hausen.** 1990. The adeno-associated virus *rep* gene suppresses herpes simplex virus-induced DNA amplification. J. Virol. **64:**3012–3018.
25. **Hermonat, P. L., M. A. Labow, R. Wright, K. I. Berns, and N. Muzyczka.** 1984. Genetics of adeno-associated virus: isolation and preliminary characterization of adeno-associated virus type 2 mutants. J. Virol. **51:**329–339.
26. **Hölscher, C., J. A. Kleinschmidt, and A. Bürkle.** 1995. High level expression of adeno-associated virus (AAV) Rep78 and Rep68 protein is sufficient for infectious-particle formation by a *rep*-negative AAV mutant. J. Virol. **69:** 6880–6885.
27. **Hörer, M., S. Weger, K. Butz, F. Hoppe-Seyler, C. Geisen, and J. A. Kleinschmidt.** 1995. Mutational analysis of adeno-associated virus Rep protein-mediated inhibition of heterologous and homologous promoters. J. Virol. **69:**5485–5496.
28. **Hunter, L. A., and R. J. Samulski.** 1992. Colocalization of adeno-associated virus rep and capsid proteins in the nuclei of infected cells. J. Virol. **66:**317–324.
29. **Im, D. S., and N. Muzyczka.** 1989. Factors that bind to adeno-associated virus terminal repeats. J. Virol. **63:**3095–3104.
30. **Ishii, N., A. Nakanishi, M. Yamada, M. H. Macalalad, and H. Kasamatsu.** 1994. Functional complementation of nuclear targeting-defective mutants of simean virus 40 structural proteins. J. Virol. **68:**8209–8216.
31. **Janik, J. E., M. M. Huston, K. Cho, and J. A. Rose.** 1989. Efficient synthesis of adeno-associated virus structural proteins requires both adenovirus DNA binding protein and VA I RNA. Virology **168:**320–329.
32. **Johnson, F. B.** 1984. Parvovirus proteins, p. 259–295. *In* K. I. Berns (ed.), The parvoviruses. Plenum Publishing Corp., New York, N.Y.
33. **Johnson, F. B., H. L. Ozer, and M. D. Hoggan.** 1971. Structural proteins of adenovirus-associated virus type 3. J. Virol. **8:**860–863.
34. **Kyöstiö, S. R., R. A. Owens, M. D. Weitzmann, B. A. Antoni, N. Chejanovsky, and B. J. Carter.** 1994. Analysis of adeno-associated virus (AAV) wild-type and mutant Rep proteins for their abilities to negatively regulate AAV p5 and p19 mRNA levels. J. Virol. **68:**2947–2957.
35. **Labow, M. A., P. L. Hermonat, and K. I. Berns.** 1986. Positive and negative autoregulation of the adeno-associated virus type 2 genome. J. Virol. **60:** 251–258.
36. **Laskey, R. A., M. P. Fairman, and J. J. Blow.** 1989. S phase of the cell cycle. Science **246:**609–614.
37. **Laughlin, C. A., J.-D. Tratschin, H. Coon, and J. B. Carter.** 1983. Cloning of infectious adeno-associated virus genomes in bacterial plasmids. Gene **23:** 65–73.
38. **McCarty, D. M., M. Christensen, and N. Muzyczka.** 1991. Sequences required for coordinate induction of adeno-associated virus p19 and p40 promoters by Rep protein. J. Virol. **65:**2936–2945.
39. **McIntosh, J. R., and M. P. Koonce.** 1989. Mitosis. Science **246:**622–628.
40. **Mittnacht, S., and R. A. Weinberg.** 1991. G1/S phosphorylation of the retinoblastoma protein is associated with an altered affinity for the nuclear compartment. Cell **65:**381–393.
41. **Muzyczka, N.** 1992. Use of adeno-associated virus as a general transduction vector for mammalian cells. Curr. Top. Microbiol. Immunol. **158:**97–129.
42. **Myers, M. W., and B. J. Carter.** 1980. Assembly of adeno-associated virus. Virology **102:**71–82.
43. **Nakamura, H., T. Morita, and C. Sato.** 1986. Structural organizations of replicon domains during DNA synthetic phase in the mammalian nucleus. Exp. Cell Res. **165:**291–297.
44. **Nakayasu, H., and R. Berezney.** 1989. Mapping replicational sites in the eucaryotic cell nucleus. J. Cell Biol. **108:**1–11.
45. **Oleksiewicz, M. B., F. Costello, M. Huhtanen, J. B. Wolfinbarger, S. Alexandersen, and M. E. Bloom.** 1996. Subcellular localization of aleutian mink disease parvovirus proteins and DNA during permissive infection of Crandell feline kidney cells. J. Virol. **70:**3242–3247.
46. **Ornelles, D. A., and T. Shenk.** 1991. Localization of the adenovirus early region 1B 55-kilodalton protein during lytic infection: association with nuclear viral inclusions requires the early region 4 34-kilodalton protein. J. Virol. **65:**424–429.
47. **Pombo, A., J. Ferreira, E. Bridge, and M. Carmo-Fonseca.** 1994. Adenovirus replication and transcription sites are spatially separated in the nucleus of infected cells. EMBO J. **13:**5075–5085.
48. **Prasad, K. M., and J. P. Trempe.** 1995. The adeno-associated virus Rep78 protein is covalently linked to viral DNA in a preformed virion. Virology **214:**360–370.
49. **Quinlan, M. P., L. B. Chen, and D. M. Knipe.** 1984. The intranuclear localization of a herpes simplex virus DNA-binding protein is determined by the status of viral DNA replication. Cell **36:**857–868.
50. **Redemann, B. E., E. Mendelson, and B. J. Carter.** 1989. Adeno-associated virus rep protein synthesis during productive infection. J. Virol. **63:**873–882.
51. **Richardson, W. D., and H. Westphal.** 1981. A cascade of adenovirus early functions is required for expression of adeno-associated virus. Cell **27:**133–141.
52. **Rose, J. A., J. V. Maizel, J. K. Inman, and A. J. Shatkin.** 1971. Structural proteins of adeno-associated viruses. J. Virol. **8:**766–770.
53. **Ruffing, M., H. Zentgraf, and J. A. Kleinschmidt.** 1992. Assembly of viruslike particles by recombinant structural proteins of adeno-associated virus type 2 in insect cells. J. Virol. **66:**6922–6930.
54. **Shaw, P. J., and E. G. Jordan.** 1995. The nucleolus. Annu. Rev. Cell Dev. Biol. **11:**93–121.
55. **Singer, I.I., and S. L. Rhode.** 1978. Ultrastructural studies of H-1 parvovirus replication. VI. simultaneous audioradiographic and immunochemical intranuclear localization of viral DNA synthesis and protein accumulation. J. Virol. **25:**349–360.
56. **Singer, I.I., and H. W. Toolan.** 1975. Ultrastructural studies of H-1 parvovirus replication. I. Cytopathology produced in human NB epithelial cells and hamster embryo fibroblasts. Virology **65:**40–54.
57. **Snyder, R. O., R. J. Samulski, and N. Muzyczka.** 1990. In vitro resolution of covalently joined AAV chromosome ends. Cell **60:**105–113.
58. **Spector, D. L.** 1993. Macromolecular domains within the cell nucleus. Annu. Rev. Cell Biol. **9:**265–315.
59. **Staufenbiel, M., W. Deppert.** 1983. Different structural systems of the nucleus are targets for SV40 large T antigen. Cell **33:**173–181.
60. **Steinbach, S., A. Wistuba, T. Bock, and J. A. Kleinschmidt.** Assembly of adeno-associated virus type 2 (AAV-2) capsids in vitro. Submitted for publication.
61. **Thomas, J. O., and R. D. Kornberg.** 1975. An octamer of histones in chromatin and free in solution. Proc. Natl. Acad. Sci. USA **72:**2626–2630.
62. **Tratschin, J. D., I. L. Miller, and B. J. Carter.** 1984. Genetic analysis of adeno-associated virus: properties of deletion mutants constructed in vitro and evidence for an adeno-associated virus replication function. J. Virol. **51:**611–619.
63. **Tratschin, J. D., J. Tal, and B. J. Carter.** 1986. Negative and positive regulation in trans of gene expression from adeno-associated virus vectors in mammalian cells by a viral *rep* gene product. Mol. Cell. Biol. **6:**2884–2894.
64. **Walton, T. H., P. T. Moen, E. Fox, and J. W. Bodnar.** 1989. Interactions of minute virus of mice and adenovirus with host nucleoli. J. Virol. **63:**3651–3660.
65. **Weitzman, M. D., K. J. Fisher, and J. M. Wilson.** 1996. Recruitment of wild-type and recombinant adeno-associated virus into adenovirus replication centers. J. Virol. **70:**1845–1854.
66. **Wilcock, D., and D. P. Lane.** 1991. Localization of p53, retinoblastoma and host replication proteins at sites of viral replication in herpes-infected cells. Nature **349:**429–431.
67. **Wistuba, A., S. Weger, A. Kern, and J. A. Kleinschmidt.** 1995. Intermediates of adeno-associated virus type 2 assembly: identification of soluble complexes containing Rep and Cap proteins. J. Virol. **69:**5311–5319.
68. **Xing, Y., C. V. Johnson, P. R. Dobner, and J. B. Lawrence.** 1993. Higher level organization of individual gene transcription and RNA splicing. Science **259:**1326–1330.